Wei, L., Agarwal, U., Stark, N., and Sabo, R. 2017, May. "Nanocomposites From Lignin-Containing Cellulose Nanocrystals and Poly(Lactic Acid)" ANTEC® 2017 - Anaheim, California, USA May 8-10, 2017. [On-line]. Society of Plastics Engineers, ISBN: 978-0-692-88309-9,

NANOCOMPOSITES FROM LIGNIN-CONTAINING CELLULOSE NANOCRYSTALS AND POLY(LACTIC ACID)

Liqing Wei, Umesh Agarwal, Nicole Stark, and Ronald Sabo
USDA Forest Service, Forest Products Laboratory, Madison, WI 53726

Abstract

Utilizing lignin-containing cellulose nanocrystals (HLCNCs) as reinforcing agents to poly(lactic acid) (PLA) for nanocomposites was studied for the first time. The PLA/HLCNCs nanocomposites were prepared by extrusion and injection molding. The freeze-dried HLCNCs showed micron scale agglomerates. As indicated by the water contact angle measurements, the HLCNCs were more hydrophobic than dealkaline lignin and traditional, lignin-free CNCs derived from high cellulose content wood pulp. Thermogravimetric analysis (TGA) showed that the HLCNCs started to degrade at about 300°C. The thermal stability of nanocomposites was slightly lower than neat PLA. The Young's modulus of nanocomposites containing 1%, 2% and 5% CNCs was improved by 21.0%, 18.4% and 17.7%, respectively, while the strain at break was improved by 73.2%, 63.4%, and 54.9% compared to neat PLA. The nanocomposites (PLA/2%HLCNC) exhibited increased microductility and plastic deformation over neat PLA during tensile test. No statistically significant changes in the tensile strength were found with HLCNC addition. The results provide some practical and fundamental insight of PLA/HLCNCs nanocomposites to be used for flexible packaging films. Future work to improve the dispersion of HLCNCs in the PLA matrix as well as in the CNC drying approach is suggested.

Introduction

Biobased plastics (bioplastics) attract extensive attention as sustainable alternatives to petroleum-based polymers. Bioplastics have been used for disposable items, such as packaging, cutlery, cups, and straws. Poly(lactic acid) (PLA) is a transparent bioplastic produced from corn starch, tapioca roots, and sugarcane [1]. Biodegradable PLA can be used for compost bags, nonwoven fabrics, mulch film, and sandbag [1]. The mechanical properties of PLA are significantly influenced by stereochemistry. Both poly-L-lactic acid (PLLA) and poly-D-lactic acid (PDLA) are hard materials with tensile moduli of about 2.7 GPa, tensile strengths of 50 to 70 MPa, elongations at break of 4%, flexural moduli of 5 GPa, and flexural strengths of 100 MPa [1].

However, compared to conventional polyolefins (PE/PP), the brittleness of PLA leads to relatively poor mechanical performance, e.g. poor flexibility/ductility. Therefore, options to modify PLA to improve the thermal and mechanical properties of PLA-based products are needed. Combining PLA with the other bio-components can result in a completely biodegradable composite (or biocomposite), in which PLA plays the role of matrix material while the other material performs as filler or reinforcement. Due to their useful properties, low cost and renewability, various biofibers (e.g., hemp, flax, or other bast fibers; agricultural waste, starch, recycled paper fibers or wood fibers) as well as cellulose and lignin have been incorporated as reinforcing agents in PLA [2].

Recently, cellulose nanomaterials have gained significant attention as reinforcement materials in polymer matrices. There are primarily two forms of plant-derived cellulose nanomaterials: cellulose nanocrystals (CNCs) and cellulose nanofibrils (CNFs). CNCs are also known as cellulose whiskers, nanowhiskers, or nanorods. The process to isolate CNCs from a given cellulose source material generally occurs in two primary steps. The first step is the purification of the source material (e.g., cotton, ramie fibers, algae, bleached wood pulp, bacterial cellulose, or tunicate) to remove most of the non-cellulose components including lignin, hemicellulose, extractives, proteins, and inorganic impurities. The second step is to obtain CNCs by a controlled acid hydrolysis in which the amorphous regions of the cellulose are removed [3]. The degree of polymerization of the rod-like acid-resistant CNCs is highly dependent on the cellulose sources. On the other hand, the dimensions (length and diameter), crystallinity, mechanical properties and surface chemistry of CNCs vary with both cellulose source as well as preparation conditions. CNCs have advantages such as high specific surface area (150-170 m^2/g), crystallinity (54%-90%) and modulus (120-170 GPa) [2,3], which are well beyond that of traditional cellulose fibers.

As is the case with cellulose materials in general, CNCs are hydrophilic due to the abundant hydroxyl groups on their surfaces. In composites, poor interaction and compatibility between CNCs and hydrophobic polymer matrices lead to poor stress transfer [2,4,5]. Another major limitation of CNCs as reinforcing agents is the ready agglomeration of freeze-dried CNCs and their small aspect ratio (length/diameter). This almost always results in CNCs as fillers rather than a true reinforcement of the polymer matrix. Hence, water-soluble matrix polymers, such as poly(vinyl alcohol) and polyethylene oxide [6,7], have been commonly used to prepare CNC

nanocomposites. Although various modifications have been attempted to improve the hydrophobicity of CNCs [8,9] and, therefore, its compatibility with the PLA matrix, the processes used are usually costly and involve toxic chemicals, which could be an impediment to the practical applications of CNC nanocomposites.

In addition to cellulose, the other major component of lignocellulosic biomass is lignin. Lignin is a complex, three-dimensional aromatic polymer that contributes to the various properties of plant cell walls, including the mechanical resistance, hydrophobicity, and dimensional stability. Lignin can be potentially used as adhesives, additives in composites, and an aromatic source for polyurethane synthesis [2]. Moreover, lignin can absorb UV light and therefore, transparent coatings with controlled UV-absorbent properties have been developed [10]. However, during the conventional CNC production process, lignin is always removed from lignocellulosic starting materials and discarded as a residue or burnt.

In this study, the lignin was retained in the CNCs, which were produced directly from heat-treated wood fibers. This resulted in CNCs that contained lignin (HLCNCs). The freeze-dried HLCNCs were compounded with PLA via extrusion and injection molding. Ultimately, our objective was to develop HLCNCs with higher hydrophobicity than conventional (i.e. lignin-free) CNCs, which would then have a greater potential to be used as reinforcing agents in a hydrophobic PLA polymer matrix. The more hydrophobic HLCNCs are expected to be helpful in addressing the challenge of CNC/PLA interfacial bonding.

Experimental

Materials

PLA pellets were obtained from NatureWorks LLC (Minnetonka, MN). The PLA had a density of 1.24g/cm^3. PLA pellets were Wiley milled to powder that passed through a 0.5mm screen and were vacuum-dried for 24 hours prior to use.

Preparation of HLCNCs

The HLCNCs were produced from aspen wood fibers via two major steps. First, the fibers were heat-treated at 200°C and then were treated with 64% sulfuric acid (under vacuum) at 45°C followed by 1h reaction with constant stirring at atmospheric pressure and under a nitrogen blanket. The hydrolysis was quenched by diluting with deionized water to approximately a 20-fold volume of the initial suspension, followed by neutralization with a sodium hydroxide solution (5wt%). The resulting suspension was further diluted and allowed to settle overnight. The solution was decanted and the suspended solids were dialyzed against reverse osmosis water for one week. The dialyzed suspension was treated with an ultrasonic probe followed by centrifugation and concentration of the CNCs suspended in the supernatant using a rotary evaporator. Tert-butanol was added to the approximately 4wt% CNC suspension for solvent exchange, which was then frozen in liquid nitrogen and freeze-dried to obtain lignin-containing cellulose nanocrystals (HLCNC). The morphology and dimensions of HLCNCs before freeze-drying were investigated by transmission electron microscopy (TEM). The HLCNC suspension was deposited on a carbon coated Formvar film (300 mesh), and then stained with 2% aqueous uranyl acetate. The samples were imaged using a Philips CM100 TEM (Philips/FEI Corporation, Holland) at an accelerating voltage of 100kV. Scanning electron microscopy (SEM) was used to study the morphology of the HLCNCs after freeze-drying.

Nanocomposites Preparation

The dry blend of PLA and freeze-dried HLCNC (1, 2, and 5 wt%) were molded using a microcompounder and microinjection molder (DSM Xplore system, DSM Research, Geleen, The Netherlands). Microcompounder barrel temperatures were set at 185°C and the screw speed was 100RPMs. A nitrogen blanket was used to minimize degradation. After compounding for 2 mins, the extrudates were collected and injection molded into Type V tensile specimens at 105°C at 10 bars of pressure for 30 seconds.

Characterization of Nanocomposites

The surface hydrophilicity of HLCNC was evaluated by contact angle measurements using a KSV Attension Theta Lite Optical Tensiometer. HLCNC powder was compression molded into discs (12 mm Ø × 1.5 mm) at 20MPa using a hydraulic press (Carver). The static contact angle between a water droplet and the CNC disc was measured. Contact angles of a normal CNC without heat treatment and a dealkaline lignin (TCI, Tokyo, Japan) were measured as comparisons. The lignin-free CNC (SCNC) was produced from a high-purity cellulose pulp in the Forest Products Laboratory's nanocellulose pilot plant via sulfuric acid hydrolysis [11,12].

The thermal stability of HLCNCs, PLA and nanocomposites were investigated by thermogravimetric analysis (TGA). Measurements were conducted on a sample (3-5 mg) using a PerkinElmer Pyris 1.0 analyzer at a heating rate of 20 $^{\circ}$C/min under N_2 atmosphere (20 mL/min).

Tensile properties were measured according to ASTM standard D638-10 with a crosshead speed of 1 mm/min. The test was performed on an Instron 5865

system (Instron Engineering Corp., MA) equipped with a 500 N load cell. An MTS LX 500 noncontact laser extensometer (MTS Systems Corporation, Eden Prairie, MN) was used to measure strain. Significance in the mechanical properties differences were statistically analyzed using one-way analysis of variance (ANOVA) at an α level of 0.05 with a Tukey's test.

In order to evaluate the degree of dispersion of HLCNCs in PLA matrix, fracture surfaces after tensile testing were studied using a field emission scanning electron microscope (SEM, LEO Gemini).

Discussion

Morphology of Cellulose Nanocrystals

The TEM image of HLCNC solution (Figure 1) shows discrete cellulose crystals of fairly low aspect ratios. Image analysis yielded estimates of crystal lengths (L) and diameters (d) of 4 to 21 nm and 35 to 230 nm, respectively, and an average aspect ratio (L/d) of 13. In addition, nano-scale lignin particles with diameters ranging from 2 to 22 nm are present in the HLCNC sample as well.

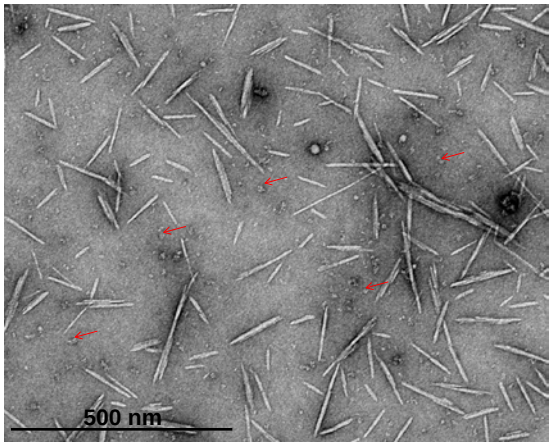

Figure 1. TEM of HLCNCs. Some nanolignin particles are shown by arrows.

The SEM micrograph of freeze-dried HLCNC is shown in Figure 2. The presence of agglomerated CNC (lamella/sheet like) originated from the hydrogen-bonding and van der Waals forces during the freeze-drying process.

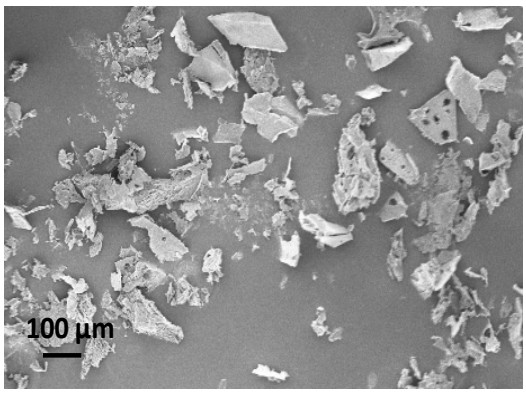

Figure 2. SEM micrograph of freeze-dried HLCNC.

CNC Surface Hydrophilicity

CNCs are commonly produced via sulfuric acid hydrolysis followed by a neutralization step with a sodium hydroxide solution. This results in very hydrophilic CNC surfaces (Figure 3, SCNC). Lignin is more hydrophobic in nature than cellulose [13], thus giving a higher water contact angle (Figure 3). Lignin-containing CNCs (HLCNCs) were successfully derived from heat-treated aspen fibers. The HLCNC surfaces are more hydrophobic than dealkaline lignin and SCNC. Thus, better interfacial bonding between the HLCNC and hydrophobic polymer matrix is expected.

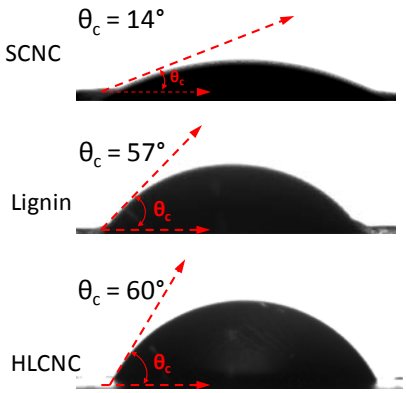

Figure 3. A water drop on the surfaces of SCNC, dealkaline lignin and HLCNC after 3 seconds.

Thermal Stability

The freeze-dried HLCNCs had darker color (Figure 4), likely due to the presence of lignin and the heat treatment, because lignin can be degraded through the whole heating scan (250-500 °C) [14]. Although nitrogen blanketing, relatively low extrusion/molding temperatures, and short processing times were used, HLCNCs could degrade somewhat during melt processing. However, how much of the color darkening for nanocomposites is due to HLCNC degradation is not clear.

Figure 4. Freeze-dried HLCNCs and injection molded nanocomposites specimens

The comparison of the onset temperature of degradation (T_{onset}, the temperature at which materials start to lose weight) is a useful measure of thermal stability for materials. The thermal stability of starting materials as well as the nanocomposites was evaluated by the thermogravimetric analysis (TGA). The TGA weight loss curves are shown in Figure 5. The ash content at 600°C was about 36% of the original weight of the HLCNCs. This compares with about 0.4%, 0.8, and 1.8% of ash contents in the nanocomposites, containing 1%, 2%, and 5% of HLCNCs, respectively. This suggests that the PLA/HLCNCs ratios were not changed during the processing. The T_{onset} for HLCNCs is about 300°C, which is similar to the reported T_{onset} for SCNC [11]. The T_{onset} values follow the order: PLA > PLA/2%HLCNC > PLA/1%HLCNC > PLA/5%HLCNC. The thermal stability of nanocomposites was slightly lower than neat PLA, possibly due to poor dispersion and insufficient encapsulation of the agglomerates of freeze-dried HLCNCs (Figure 2) by the polymer melt.

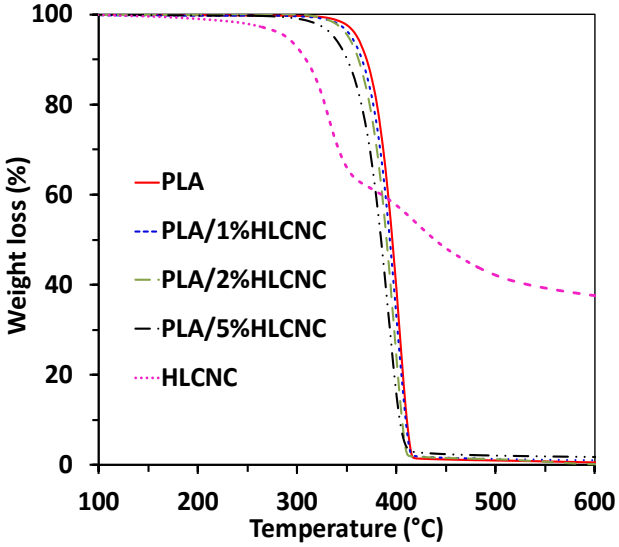

Figure 5. TGA of HLCNC, PLA, and nanocomposites.

Tensile Properties

The relatively higher aspect ratio of HLCNCs (L/d = 13) compared to that of SCNCs (L/d = 8) derived from bleached dry lap eucalyptus pulp [7], making HLCNCs better for polymer reinforcement. The tensile properties of PLA and PLA/HLCNC nanocomposites are shown in Figure 6. Compared to neat PLA, improvements in tensile modulus of 21.0%, 18.4% and 17.7% were found for PLA/1%HLNC, PLA/2%HLCNC, and PLA/5%HLCNC nanocomposites, respectively, and were 73.2%, 63.4%, and 54.9% for strain at break (ε, %). Neat PLA is considered to be a brittle polymer. Hence, the increased ε values with addition of a small amount of HLCNC results in stiffer and more ductile nanocomposites as compared to the neat PLA. However, adding more than 2% HLCNCs offers little additional advantage in modulus or strain at break. No statistically significant effect on tensile strength was found with addition of HLCNCs. The lack of reinforcement by the HLCNCs is possibly due to reduction of their aspect ratios during freeze-drying, as they are transformed from rod-like shapes to flakes through agglomeration. However, it is worth noting that our previous findings show that freeze-dried SCNC/PLA nanocomposites show even larger strength reductions compared to neat PLA [11]. Hence, it seems the freeze-dried HLCNCs perform better as a reinforcing agent than freeze-dried SCNCs, which may be due to the higher aspect ratio of freeze-dried HLCNC flakes than the SCNC flakes [11]. The tensile strength of low aspect ratio biofiber and polymer composites is more dependent on the fiber-polymer interaction (compatibility) than those with higher aspect ratios [15]. This agrees with the hydrophilicity results (Figure 3), in which the surfaces of HLCNCs are more hydrophobic than SCNCs, possibly providing better interfacial bonding at the HCNCs and hydrophobic PLA polymer matrix.

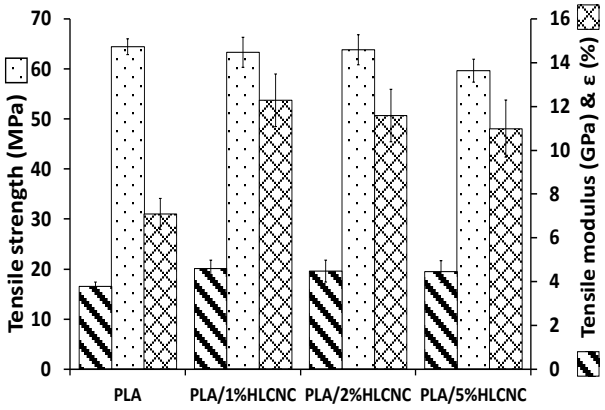

Figure 6. Tensile properties of PLA and nanocomposites.

Study of Fractured Surfaces

In order to assess the dispersion of HLCNCs in the polymer matrix and the HLCNC/polymer interface, tensile

fracture surfaces. The fracture surface of neat PLA shows less plastic deformation ascribing to its brittle nature (Figure 7a). In contrast, the nanocomposites (PLA/2%HLCNC) exhibit microductility and plastic deformation (Figure 7b, 7c and 7d). This is in agreement with its ductile fracture as demonstrated by its higher elongation at break (ε) value. There seems no apparent void at the interfaces of HLCNC flakes and polymer matrix, indicating better HLCNC/polymer interfacial bonding and improved stress transfer at the interface. However, large HLCNC agglomerates can be observed in the nanocomposites, which presumably lead to stress concentration at the large agglomerate surfaces and contribute to lower tensile strength.

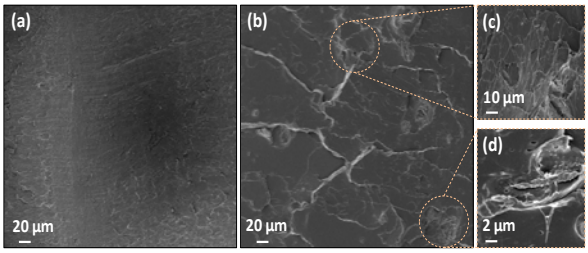

Figure 7. Fractured surfaces of (a) PLA, (b) PLA/2%HLCNC nanocomposites, and microductility of PLA can be seen in close up view (c and d).

Conclusions

Lignin-containing CNCs (HLCNCs) were successfully produced from heat-treated aspen wood fibers. Freeze-dried HLCNCs formed sheet-like agglomerates, lacking the rod-like morphology of a reinforcing agent. HLCNCs were compounded with PLA via melt-processing. HLCNCs showed improved hydrophobicity compared to traditional CNCs from high cellulose wood pulp and dealkaline lignin. Higher Young's modulus and elongation at break values were obtained by addition of 2% HLCNCs to PLA. Further significant improvement was not observed when HLCNC loading was increased from 2% to 5%. No statistically significant changes in tensile strength were found when HLCNCs were added to PLA. Although better interfacial bonding of more hydrophobic HLCNCs and hydrophobic PLA matrix may have been achieved, poor dispersion of large aggregates of HLCNCs in the PLA matrix still seem to be a complication of freeze-drying HLCNCs. However, as reinforcing agent the HLCNCs perform better than lignin-free CNCs, contributing to higher aspect ratio of freeze-dried flakes. Further investigation into the better dispersion of HLCNCs into the PLA matrix is currently underway. For example, wet compounding of never-dried HLCNC suspensions and PLA powder is being investigated. This research could potentially broaden the application of CNC nanocomposites in biodegradable and UV-absorbent but transparent packaging products and facilitate the commercialization of cellulose nanomaterials.

Acknowledgement

The project was supported by the Public-Private Partnership for Nanotechnology (P3Nano) US Endowment for Forestry and Communities, Inc. The authors would like to acknowledge Rick Reiner, Engineering Mechanics Laboratory of the Forest Products Laboratory, for preparing the freeze-dried SCNCs.

References

1. R. Auras, L.-T. Lim, S.M. Selke, and H. Tsuji. John Wiley & Sons, Inc.: Hoboken, New Jersey. (2010)
2. L. Wei, and A. McDonald. *Materials, 9*, 303 (2016).
3. R.J. Moon, S. Beck, and A.W. Rudie. Cellulose nanocrystals – a material with unique properties and many potential applications In *Production and applications of cellulose nanomaterials*, Postek, M.T.; Moon, R.J.; Rudie, A.W.; Bilodeau, M.A., Eds. TAPPI Press: Peachtree Corners, GA, 2013; pp 9.
4. L. Wei, N.M. Stark, and A.G. McDonald. *Green Chem., 17*, 4800 (2015).
5. L. Wei, A.G. McDonald, and N.M. Stark. *Biomacromolecules, 16*, 1040 (2015).
6. F. Ansari, M. Salajková, Q. Zhou, and L.A. Berglund. *Biomacromolecules, 16*, 3916 (2015).
7. X. Xu, F. Liu, L. Jiang, J.Y. Zhu, D. Haagenson, and D.P. Wiesenborn. *ACS Appl. Mater. Interfaces, 5*, 2999 (2013).
8. E. Espino-Pérez, J. Bras, V. Ducruet, A. Guinault, A. Dufresne, and S. Domenek. *Europ. Polym. J., 49*, 3144 (2013).
9. A. Pei, Q. Zhou, and L.A. Berglund. *Compos. Sci. Technol., 70*, 815 (2010).
10. A. Hambardzumyan, L. Foulon, B. Chabbert, and V. Aguié-Béghin. *Biomacromolecules, 13*, 4081 (2012).
11. L. Wei, N.M. Stark, R.C. Sabo, and L. Matuana. Proceedings, Forest Products Society International Convention, June 28-29, Portland, OR, (2016).
12. R. Reiner, and A. Rudie. Process scale-up of cellulose nanocrystal production to 25 kg per batch at the forest products laboratory In *Production and applications of cellulose nanomaterials*, Postek, M.T.; Moon, R.J.; Rudie, A.W.; Bilodeau, M.A., Eds. TAPPI Press: Peachtree Corners, GA, 2013; pp 21.
13. V.K. Thakur, M.K. Thakur, P. Raghavan, and M.R. Kessler. *ACS Sustainable Chem. Eng., 2*, 1072 (2014).
14. L. Wei, A.G. McDonald, C. Freitag, and J.J. Morrell. *Polym. Degrad. Stab., 98*, 1348 (2013).
15. M. Bengtsson, P. Gatenholm, and K. Oksman. *Compos. Sci. Technol., 65*, 1468 (2005).